Supporting Information

Microfluidic-based cardiovascular systems for advanced study of atherosclerosis

Huiyuan Zheng,[a,c] Lei Tai,[b] Chengbin Xu,[b] Weijiang Wang,[a] Qingming Ma,[a,*] Wentao Sun[c,*]

a. School of Pharmacy, Qingdao University, Qingdao 266071, China.
b. Pharmacy Department, Shandong Qingdao Hospital of Integrated Traditional and Western Medicine, Qingdao 266002, China.
c. School of Health and Life Sciences, University of Health and Rehabilitation Sciences, Qingdao 266113, China.

* Corresponding author.
E-mail address: qma@qdu.edu.cn (Q. Ma), sunwt@uor.edu.cn (W. Sun).

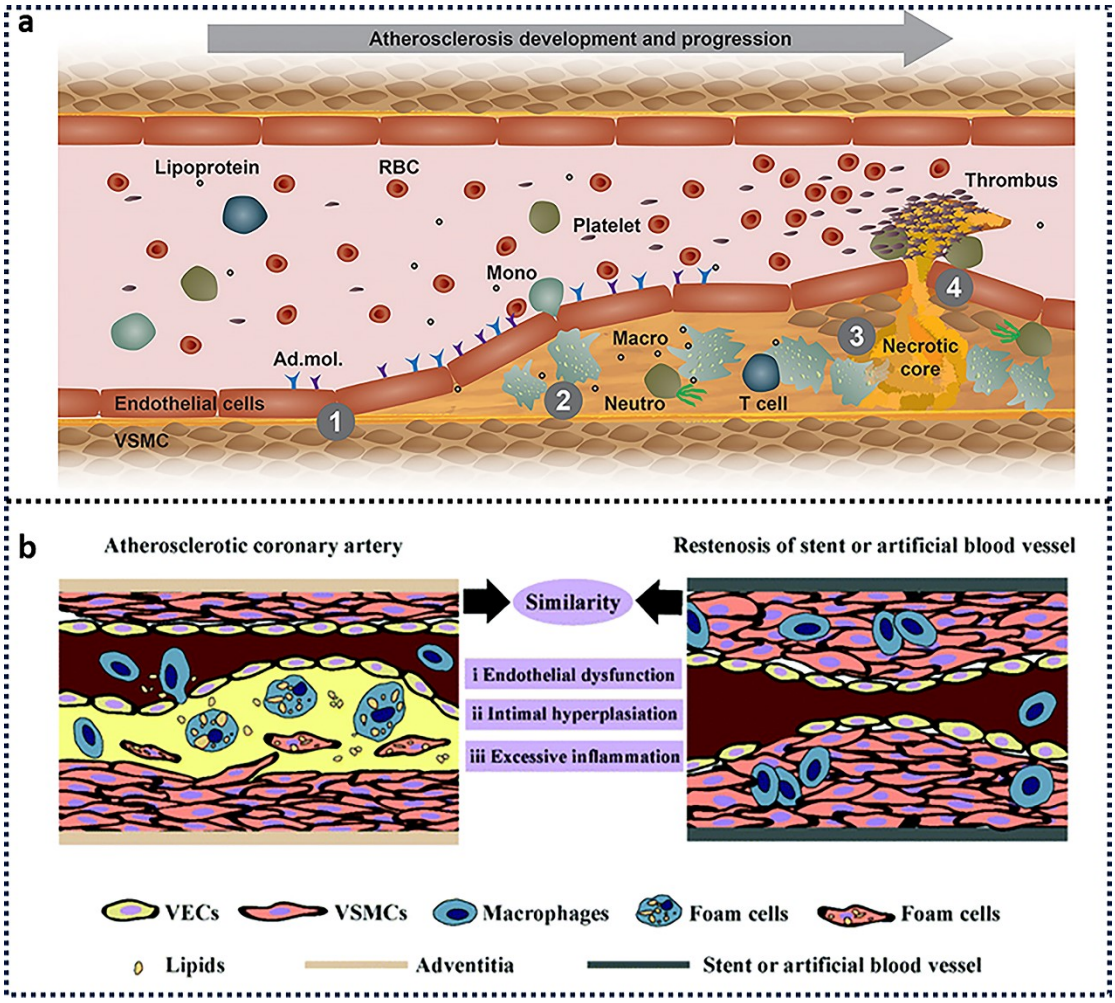

Fig. S1. Pathophysiology of AS and related diseases. (a) Models of the development and progression of AS. Reproduced from reference [1] with permission from Frontiers Media SA, copyright 2019. (b) The pathophysiology of AS and vascular restenosis. Reproduced from reference [2] with permission from The Royal Society of Chemistry, copyright 2022.

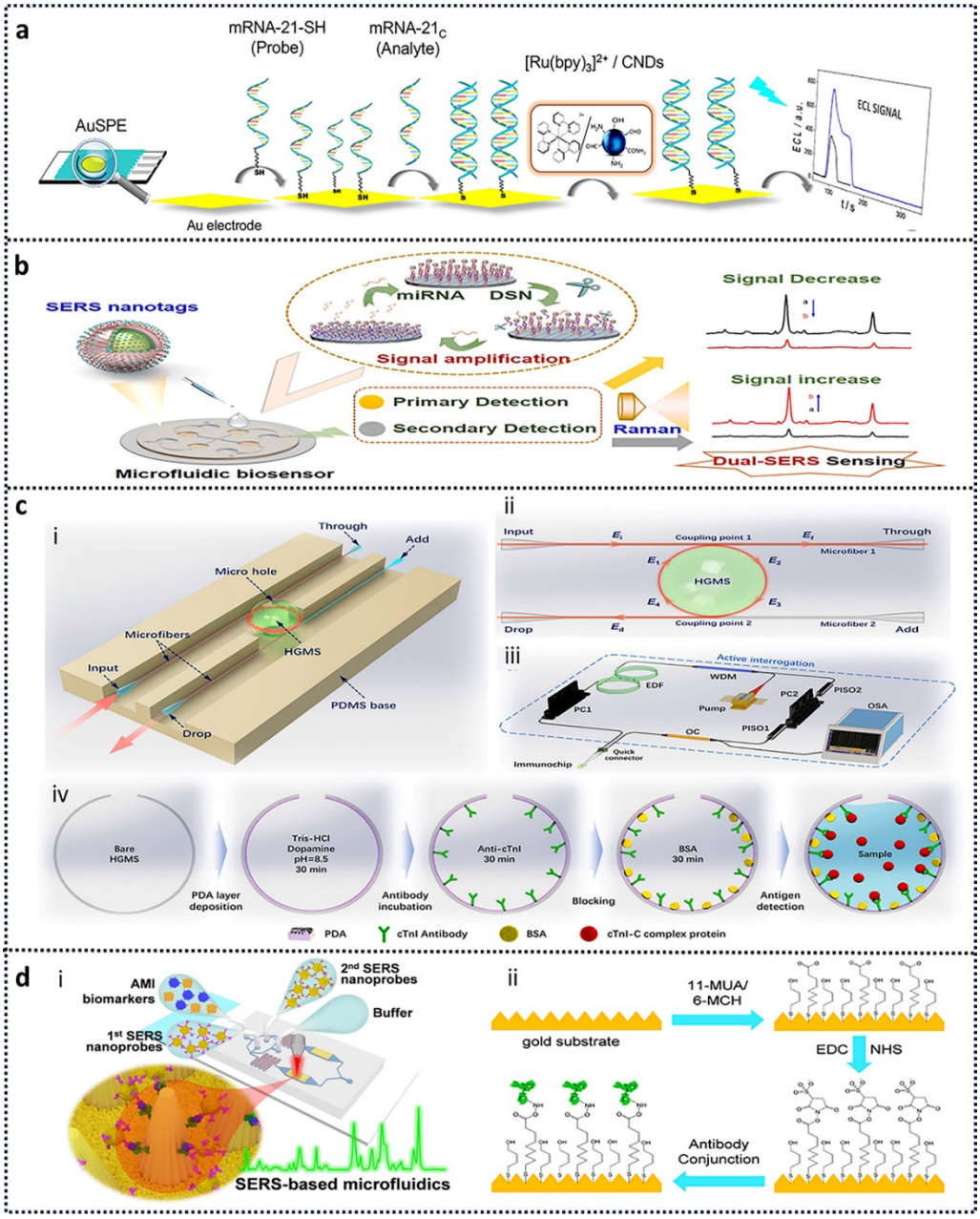

Fig. S2. Application of microfluidic systems in the detection of protein and nucleic acid cardiovascular markers. (a) Schematic illustration of DNA biosensor development: probe fixation, hybridization with analytes, and ECL detection using the $[Ru(bpy)_3]^{2+}$/CNDs system. Reproduced from reference [3] with permission from Springer Nature, copyright 2021. (b) Schematic illustration of microfluidic biosensor for the detection of miRNA-21. Reproduced from reference [4] with permission from Elsevier, copyright 2022. (c) Schematic diagram of the hollow microsphere-integrated optofluidic immunochip (i); Schematic diagram of the optical wavelength filter based on WGM microcavity in the hollow microsphere-integrated immunochip (ii); Schematic diagram of the active interrogation for WGM lasing detection (iii); Schematic of the functionalization process of the perforated HGMS (iv). Reproduced from reference [5] with permission from Elsevier, copyright 2024. (d) Schematic illustrations for the simultaneous SERS detection of CK-MB and cTnI cardiac biomarkers on the microfluidic system (i); Antibody conjugation process on PNMA substrate (ii). Reproduced from reference [6] with permission from American Chemical Society,

copyright 2022.

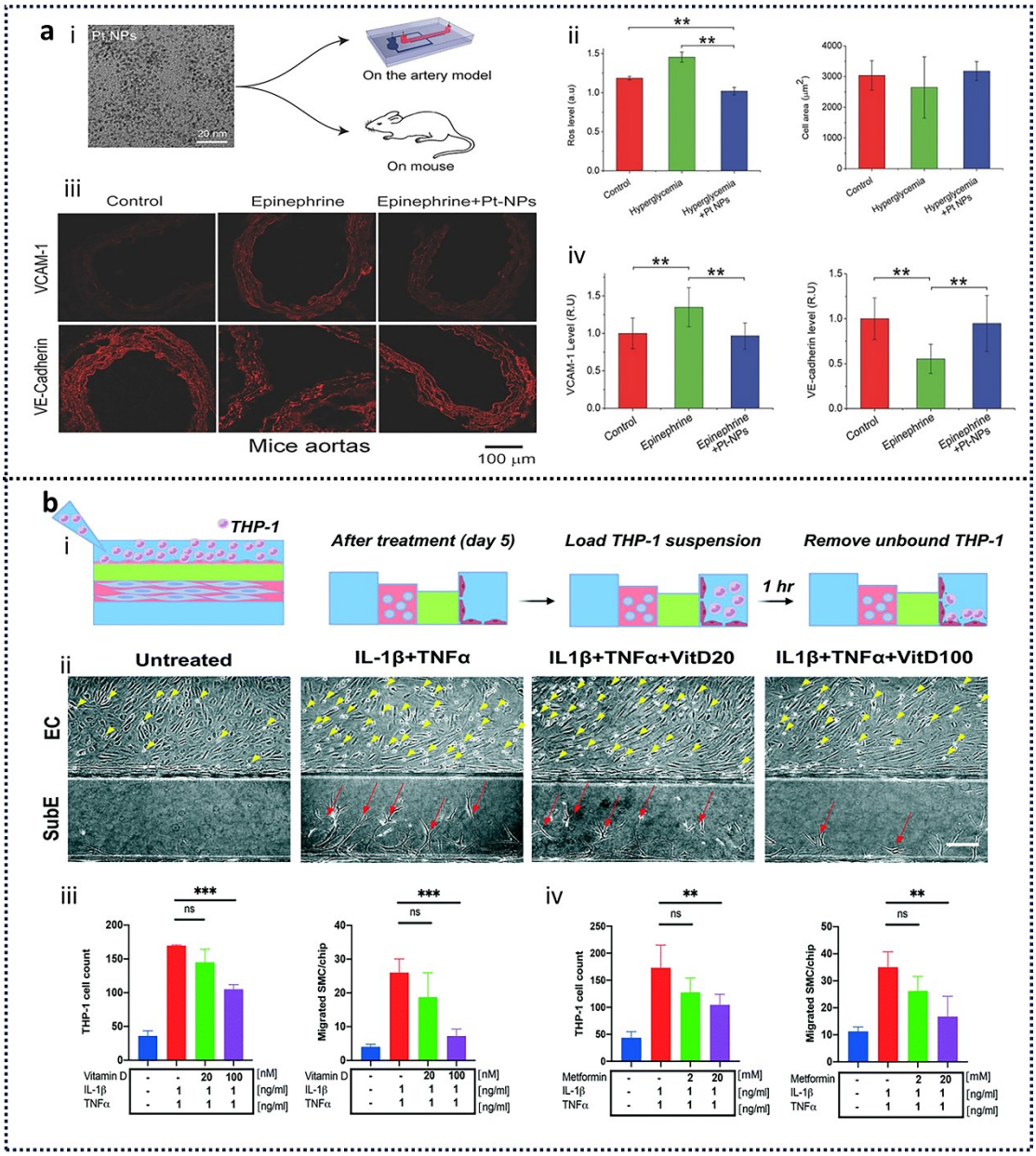

Fig. S3. Representative microfluidic-based AS models for drug discovery. (a) TEM image of the Pt-NPs and schematic diagram of efficacy evaluation of Pt-NPs on AS microfluidic models and mice (i); The on-chip experiments show the changes of ROS level and EC area before and after Pt-NPs treatment (ii); Distribution (iii) and expression levels (iv) of VCAM-1 and VE-cadherin in the aortas of mice in different groups. Scale bars: 100 μm (iii). Reproduced from reference [7] with permission from WILEY-VCH Verlag GmbH, copyright 2016. (b) Experimental procedure for the on-chip monocyte adhesion assay (i); Brightfield images of chips treated with different reagents (ii); Quantification of THP-1 cells adhesion and SMC migration for vitamin D(iii) and metformin studies(iv). Scale bar: 200 μm (ii). Reproduced from reference [8] with permission from The Royal Society of Chemistry, copyright 2021.

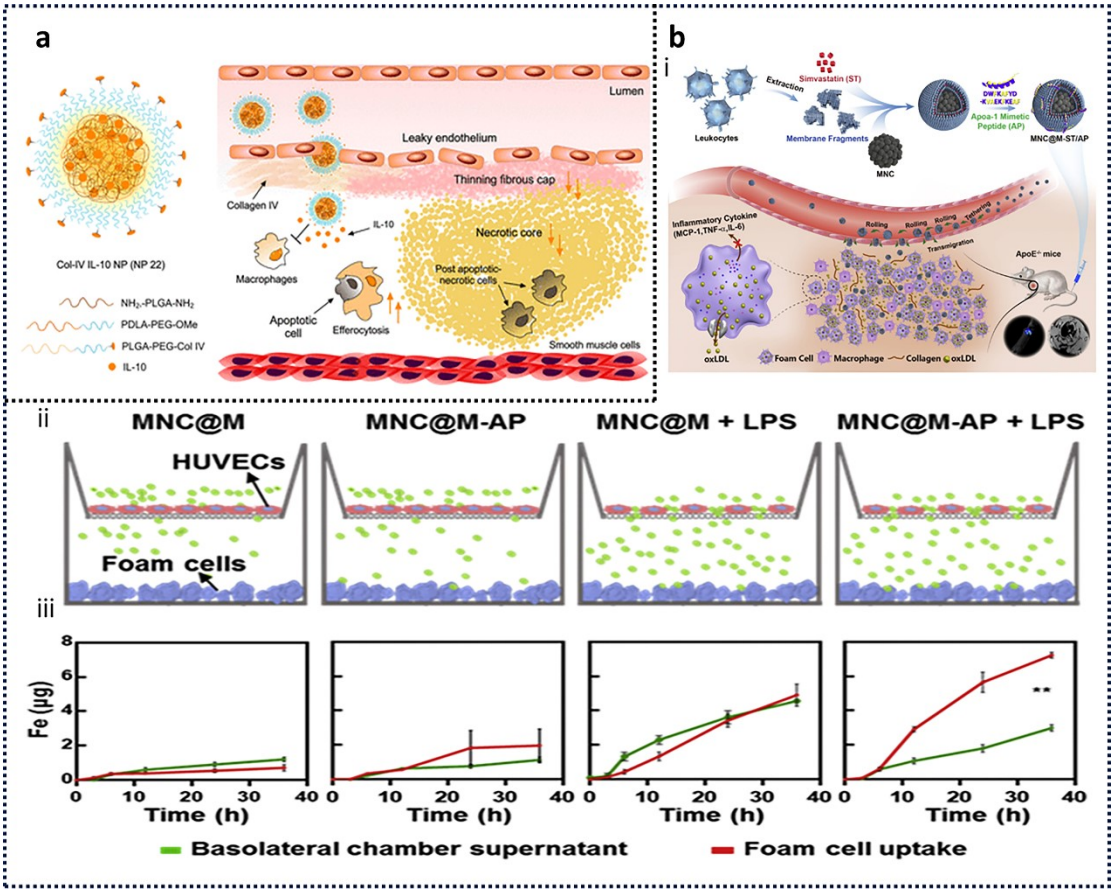

Fig. S4. Representative microfluidic-based atherosclerotic drug delivery carriers. (a) Schematic diagram of targeted anti-inflammatory nanoparticles and its application in atherosclerotic plaque inflammation. Reproduced from reference [9] with permission from American Chemical Society, copyright 2016. (b) Schematic diagram of the manufacture of biomimetic nanoparticles and their application in anti-AS (i); The established transwell models (ii); Time-dependent quantification of Fe content in the basolateral chamber supernatant or foam cells (iii). Reproduced from reference [10] with permission from Elsevier, copyright 2020.

References

[1] S. Oppi, T.F. Lüscher, S. Stein, Mouse models for atherosclerosis research—which is my line?, Frontiers in cardiovascular medicine 6 (2019) 46.

[2] X. Wang, B. Gao, Y. Feng, Recent advances in inhibiting atherosclerosis and restenosis: From pathogenic factors, therapeutic molecules to nano-delivery strategies, Journal of Materials Chemistry B 10(11) (2022) 1685-1708.

[3] L. Gutiérrez-Gálvez, T. García-Mendiola, C. Gutiérrez-Sánchez, T. Guerrero-Esteban, C. García-Diego, I. Buendía, M.L. García-Bermejo, F. Pariente, E. Lorenzo, Carbon nanodot–based

electrogenerated chemiluminescence biosensor for miRNA-21 detection, Microchimica Acta 188 (2021) 1-12.
[4] W. Ma, L. Liu, X. Zhang, X. Liu, Y. Xu, S. Li, M. Zeng, A microfluidic-based SERS biosensor with multifunctional nanosurface immobilized nanoparticles for sensitive detection of MicroRNA, Analytica Chimica Acta 1221 (2022) 340139.
[5] P. Niu, J. Jiang, K. Liu, X. Zhou, S. Wang, T. Xu, T. Wang, Y. Li, Q. Yang, T. Liu, Hollow-microsphere-integrated optofluidic immunochip for myocardial infarction biomarker microanalysis, Biosensors and Bioelectronics 248 (2024) 115970.
[6] R. Gao, Y. Mao, C. Ma, Y. Wang, H. Jia, X. Chen, Y. Lu, D. Zhang, L. Yu, SERS-Based immunoassay of myocardial infarction biomarkers on a microfluidic chip with plasmonic nanostripe microcones, ACS Applied Materials & Interfaces 14(50) (2022) 55414-55422.
[7] W. Zheng, R. Huang, B. Jiang, Y. Zhao, W. Zhang, X. Jiang, An early-stage atherosclerosis research model based on microfluidics, Small 12(15) (2016) 2022-2034.
[8] C. Su, N.V. Menon, X. Xu, Y.R. Teo, H. Cao, R. Dalan, C.Y. Tay, H.W. Hou, A novel human arterial wall-on-a-chip to study endothelial inflammation and vascular smooth muscle cell migration in early atherosclerosis, Lab on a Chip 21(12) (2021) 2359-2371.
[9] N. Kamaly, G. Fredman, J.J.R. Fojas, M. Subramanian, W.I. Choi, K. Zepeda, C. Vilos, M. Yu, S. Gadde, J. Wu, Targeted interleukin-10 nanotherapeutics developed with a microfluidic chip enhance resolution of inflammation in advanced atherosclerosis, ACS nano 10(5) (2016) 5280-5292.
[10] G. Wu, W. Wei, J. Zhang, W. Nie, L. Yuan, Y. Huang, L. Zuo, L. Huang, X. Xi, H.-Y. Xie, A self-driven bioinspired nanovehicle by leukocyte membrane-hitchhiking for early detection and treatment of atherosclerosis, Biomaterials 250 (2020) 119963.